

The quantum electrical triangle

BY JOHN GALLOP

*Quantum Detection Group, National Physical Laboratory, Queens Road
Teddington, Middlesex TW11 0LW, UK
(john.gallop@npl.co.uk)*

The past 35 years have seen the development of an unexpected plethora of quantum electrical standards based on just two fundamental constants, e and h . First came a voltage standard based on the Josephson a.c. effect, in terms of which most maintained primary standards of voltage are defined. This was followed a decade later by the quantized Hall effect, based on the von Klitzing constant which allows the ohm to be maintained very precisely. It became clear 20 years ago that there is also a possible quantum current standard. This third standard has yet to play a full part in practical electrical metrology. However, recent developments suggest that there are many different possible manifestations in which such a current standard might be realized.

The three quantum standards, taken together, define the quantum electrical triangle of standards which would allow the units to be realized in terms of different combinations of e and h . We summarize the very different physics behind the three standards, reviewing the present state of development in all three. Implications for the future are also considered, especially relating to ultra-low temperature, nanoscale and truly quantum mechanical versions of the standards.

Keywords: Josephson; quantum Hall; single electron standard

1. Introduction

This paper reviews developments in quantum electrical standards (voltage, resistance and current) over the past 35 years since the introduction of the Josephson voltage standard. All three standards involve quantum effects in cryogenic condensed matter systems but each is very different in detail. The physics underlying each standard is first reviewed and the three implementations contrasted. Then the paper concentrates on the variety of possible realizations of quantum current standards, none of which has yet achieved a level of accuracy to test the self-consistence of values of h and e derived from the quantum electrical standards alone. Finally the implications of progress towards nanoscale circuits and the demands of quantum electronic measurements are considered, along with their likely impact on future developments.

One contribution of 14 to a Discussion Meeting ‘The fundamental constants of physics, precision measurements and the base units of the SI.’

2. Josephson voltage standard

Superconductivity was first observed in 1911 but it took almost five decades to provide the first microscopic theory of the effect and another decade to fully appreciate that superconductivity is a manifestation of a macroscopic quantum state. Here the important point for this discussion is that everywhere within a simple bulk superconductor there exists a single wave function describing the Cooper pair condensate Ψ which has a position dependent amplitude and phase:

$$\Psi(r) = \Psi_0(r)e^{i\vartheta}. \quad (2.1)$$

(a) Flux quantization and Josephson effects

The unique properties of the Josephson voltage standard can be rather simply explained through the description of a single superconductor by a macroscopic wave function. Both the Meissner effect and magnetic flux quantization (the quantum being $\Phi_0 = h/2e$) arise directly from the requirement that this wave function (sometimes called the order parameter) should everywhere be single valued. This flux quantization gives rise to the existence of a new type of particle the fluxon, associated with each quantum of magnetic flux, the particle may be more or less mobile. The Josephson effects exist between weakly coupled superconductor electrodes, in which Cooper pairs (the bosonic charge carriers which are formed below the superconducting transition temperature T_c and which are responsible for dissipationless currents) tunnel between them.

The archetypal Josephson junction is formed when a thin insulating barrier is introduced between two superconductors. When the junction is cooled below T_c and exposed to electromagnetic radiation of frequency, f , the direct time-independent voltage across the junction V_J assumes discrete values given by $V_J = n\phi_0/K_J$ where n is an integer which identifies a constant voltage step (the Shapiro step) in a current–voltage characteristic (IVC) and K_J is the Josephson constant. A Josephson junction can be thought of as a device which allows the passage of a single flux quantum per cycle of the applied electromagnetic field, while maintaining phase coherence between superconducting electrodes. The maximum response frequency which determines the maximum frequency or voltage to which these effects may be observed is set by the superconducting energy gap 2Δ where

$$f_{\max} \sim 2\Delta/h, \quad V_{\max} \sim \Delta/e. \quad (2.2)$$

For conventional metallic superconductors (such as Nb) the maximum voltage is around 2 mV and the maximum effective Josephson frequency is around 1 THz.

(b) Semi-classical description of the Josephson effects

The properties of a single Josephson junction can be quantitatively derived in great detail by solving the following two equations for the phase difference (ϕ)-dependent free energy $U(\phi)$ and the time dependent current through the junction, using the a.c. Josephson relationship to derive the voltage V across the junction in terms of the time dependent phase (equation (2.5)). The phase difference ϕ is just the difference in the phase of the order parameters ($\phi = \theta_1 - \theta_2$)

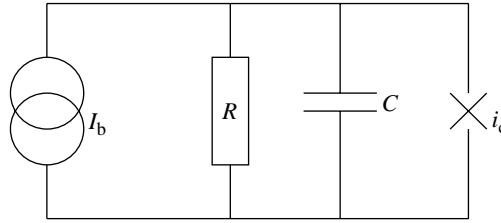


Figure 1. Schematic of current biased Josephson junction showing resistive and capacitive shunts. in the two superconductors on either side of the weak-link.

$$U(\varphi) = -\frac{\Phi_0 i_c}{2\pi} \cos(\varphi) - \Phi_0 I_b \varphi, \quad (2.3)$$

$$i_b = i_c \sin \varphi + \frac{\Phi_0}{R} \frac{d\varphi}{dt}, \quad (2.4)$$

$$V = \frac{\Phi_0}{2\pi} \frac{d\varphi}{dt}. \quad (2.5)$$

The bias current i_b is the sum of a constant part and an oscillating current representing applied microwave radiation which couples to the junction. R is an ohmic resistance which shunts the junction (see figure 1), i_c is the junction critical current—the maximum superconducting current the junction can pass before exhibiting resistance.

(c) The Josephson voltage standard

The remarkable Shapiro step structure observed in the IVC of a single Josephson junction when irradiated with microwaves led to pioneering set of experiments at the University of Pennsylvania which showed the fundamental nature of the effects and implications for evaluation of the fundamental constants (Taylor *et al.* 1969). As a result of that and much subsequent work the importance of the effect for the realization of a high precision and universal voltage standard became clear. The Josephson constant K_J is believed to be equal, to a very high degree, to the ratio $h/2e$ where h is Planck's constant and e is the electronic charge. The basis for this belief will be considered in more detail below. Assuming this relationship to be exact for now it is clear that the spacing between steps becomes

$$V = 2nef/h. \quad (2.6)$$

In January 1990 a value of $483\,597.9 \text{ GHz V}^{-1}$ was adopted for the Josephson constant K_J in SI units with a relative standard uncertainty of 8.5×10^{-8} .

The relatively small voltage which can be realized across a single junction (say a few mV) compared with the level at which most precision voltage calibrations are required (typically a few volts) meant that high precision potentiometry was initially required but ingenious developments in the 1980s led to the realization of large scale series arrays of up to 20 000 Josephson junctions which allowed up to 10 V to be realized and compared with room temperature electronic standards. The story of these developments is fascinating (see for example Kohlmann *et al.* 2003) but is outside the scope of this paper.

(d) Most accurate measurement in the world?

Since its first inception many questions have been posed concerning the accuracy of the basic a.c. Josephson relationship (equation 2.6). These ask whether the relationship is independent of frequency, voltage, temperature, the superconductor from which the junction is made and especially are the values of the fundamental constants e and h modified from their ‘free-space’ values? The only convincing answer comes from experiment (although there has also been an extensive quasi-philosophical debate which we refer to below). Tsai *et al.* (1983) tested the material independence of the Josephson voltage–frequency relationship. Two junctions made of different superconductors (Nb and In) and different coupling mechanisms (tunnel junction and weak-link). The extreme sensitivity of a superconducting quantum interference device (SQUID) detector to very small voltage differences between the junctions (when biased with same microwave frequency on the same step) allowed the material independence to be tested to one part in 10^{16} . Similar tests by the same group using two Josephson junctions separated by some 75 mm in the earth’s gravitational field have been used to demonstrate the equivalence principle for voltage measurement (Jain *et al.* 1987). This has involved using a SQUID as a null detector with a sensitivity of 10^{-22} V. A measurement which demonstrates independence of bias conditions and reproducibility from individual device to device has been done where two separate sections of a Josephson array voltage standard were intercompared and agreement found to two parts in 10^{17} (Krasnopolin *et al.* 2002). Both temperature and superconducting coupling parameter independence were demonstrated (though at a much lower level of sensitivity) by comparison between Nb Josephson junctions at 4.2 K and YBCO junctions held at 64 K, showing agreement between the Shapiro step voltages to within two parts in 10^8 (Klushin *et al.* 2002).

3. Recent developments in Josephson voltage standards

(a) Programmable Josephson arrays

There are some restrictions with fixed array voltage standards which recent developments in Josephson junction technology have attempted to address. First the induced Shapiro steps are somewhat unstable in under-damped arrays so that operation on a fixed voltage over a long time is difficult. It is also time consuming to select an arbitrary voltage. To overcome these problems programmable arrays have been fabricated (Benz *et al.* 1997). These use over-damped Josephson junctions with non-hysteretic IV characteristics. Various combinations of materials are being used to insert a normal metal shunt layer into the junctions including Nb/PdAu/Nb, NbN/TiN/NbN and Nb/Al₂O₃/Al/Al₂O₃/Nb. The overall array is divided into segments, often with a binary sequence of junctions in each. Then a specific step may be selected by choice of bias current. Figure 2 shows such a 1V array, divided into a binary sequence and consisting of 8192 junctions, allowing 14 bit resolution (Kohlmann *et al.* 2003).

(b) Josephson arbitrary waveform synthesizer

Further developments involve attempts to create a quantum-based alternating voltage standard, the Josephson arbitrary waveform synthesizer being one

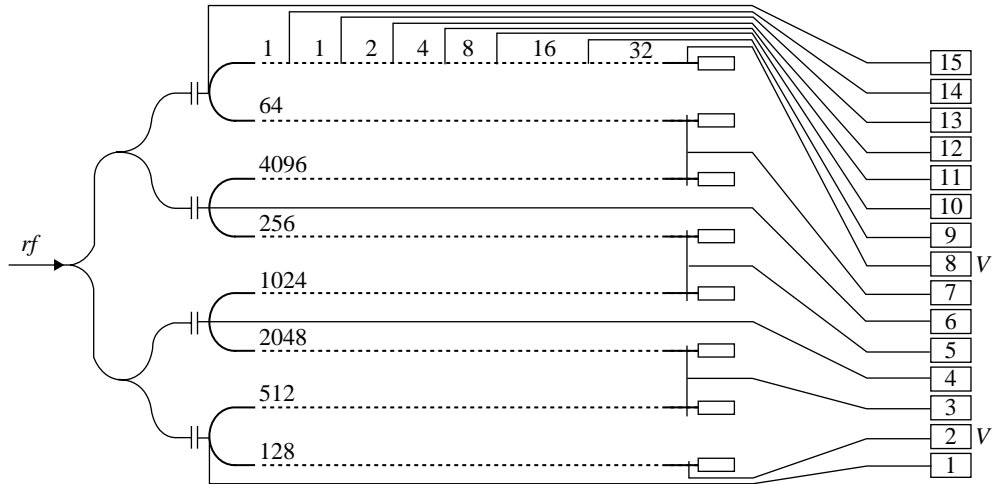


Figure 2. Schematic of Josephson programmable voltage array, showing eight parallel segments with junctions grouped in sequences from 1 to 4096 (Kohlman *et al.*).

example being developed to exploit the perfect quantization of Josephson junctions (Benz *et al.* 2001). The goal is to create a quantum-based voltage source capable of synthesizing precision arbitrary voltage waveforms for metrology and high performance applications. This will require development of nanoscale junctions but should lead to state-of-the-art low-phase noise superconducting integrated circuits. Resistively shunted junctions are used in this application too, to provide greater stability arising from heavy damping. In this case, the Josephson junction generates perfectly quantized voltage pulses when subjected to current pulses of carefully chosen amplitude. (In principle the amplitude does not need to be well defined although in practice care must be taken to select appropriate amplitude.) The time-integrated area of every Josephson pulse is precisely equal to $\hbar/2e$. Digital synthesis techniques and precise control of the timing of every pulse allows the generation of voltage waveforms with unprecedented accuracy and stability. If the input current stimulus $i(t)$ is an isolated pulse, taking the initial conditions $d\varphi/d\tau_{\text{initial}}=0$ and $\varphi_{\text{initial}}=0$ then the equilibrium solutions to the equation after the pulse, are $d\varphi/d\tau_{\text{final}}=0$ and $\varphi_{\text{final}}=2n\pi$ where n is an integer (the solutions $\varphi=(2n+1)\pi$ are non-equilibrium) regardless of the pulse parameters. The phase change φ induced by the current pulse is therefore always $2n\pi$. The instantaneous voltage across the junction is given by

$$V(t) = \frac{\hbar}{2e} \frac{d\varphi}{dt}, \quad (3.1)$$

and integrating this equation over the current pulse results in

$$\int V(t)dt = \frac{\hbar\Delta\varphi}{2e} = n\Phi_0. \quad (3.2)$$

Each pulse moves the junction phase through n wells in the ‘washboard’ potential where n depends on the pulse amplitude. Making use of this property pulse pattern generators, operating at up to 10 Gb/s, provide a sequence of

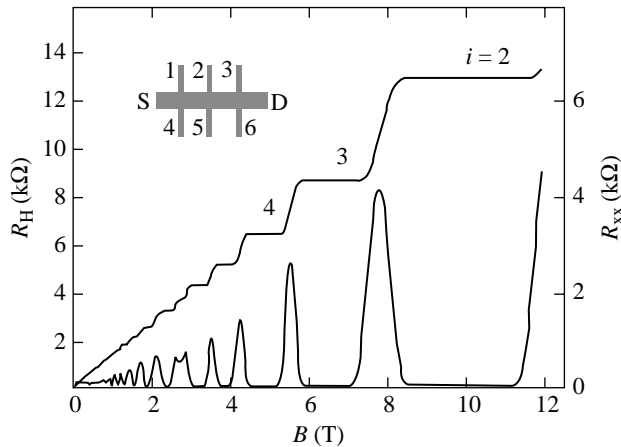


Figure 3. Quantized Hall resistance and diagonal resistance of a 2DEG in GaAs/GaAlAs heterostructure at $T=300$ mK (after Hartland *et al.*)

pulses which may be programmed to synthesize any waveform. Devices have demonstrated the best low phase noise and harmonic distortion of any synthesizer up to a frequency of around 100 kHz at present but much higher frequencies should prove accessible (Williams *et al.* 2004). At present the systems developed are limited to rather low voltages since only short arrays have been fabricated. Other applications of these devices include the quantum voltage noise source, a pseudo random noise generator for a new form of Johnson noise thermometry being developed at the National Institute of Standards and Technology (NIST) (Nam *et al.* 2003).

4. The quantized hall effect

The quantized Hall effect was discovered by von Klitzing *et al.* (1980). They demonstrated that the Hall resistance, R_H , measured in silicon metal oxide semiconductor field effect transistors (MOSFETs) at low temperatures and in high magnetic fields is quantized. Since the original discovery, the effect has been observed in various hetero-structure devices fabricated from III–V compound semi-conductors, particularly gallium arsenide, GaAs. The quantized Hall effect is most easily observed in gallium arsenide/gallium aluminium arsenide hetero-structure devices. In these, the electrons have very high mobility in a quasi-two-dimensional region of the GaAs close to the GaAs/GaAlAs interface. When contacts are attached a current I_{SD} can flow between the source (S) and drain (D) electrodes through the two-dimensional layer and potential differences between pairs of contacts. The Hall voltage, V_H is measured between opposite pairs, such as two and five. The Hall resistance, R_H , given by the ratio of V_H to I_{SD} is found to be quantized (see figure 3) and the values of the Hall resistance on the plateaus are observed to be independent of magnetic field and device geometry.

The quantized resistance values are found to be integer multiples and can be described by the equation $R_H(i) = R_K/i$ where i is an integer and $R_K = e^2/h$ is the von Klitzing constant. The simplified model described above ignores interactions

between carriers in the two-dimensional electron gas (2DEG). In reality a more sophisticated model, taking into account interactions, shows that the edges of the 2DEG in a magnetic field consists of one-dimensional channels that arise from the confining electric field at the edge of the system. The crossed electric and magnetic fields cause electrons to drift parallel to the sample boundary, creating a chiral current that travels along the edge in only one direction. In an ideal two-dimensional electron system in the quantum Hall regime, all the current flows along the edge. Quantization of the Hall resistance arises from occupation of i one-dimensional edge channels, each contributing a conductance of e^2/h . (For further details of recent developments see the preceding article in this proceedings, [von Klitzing 2005](#).)

The von Klitzing constant is believed by many theorists to be equal to the ratio h/e^2 to the highest accuracy. In January 1990, the results of measurements of the von Klitzing constant in SI units were combined with other physical measurements of h/e^2 to give a consensus value for R_K , R_{K-90} of 25 812.807 Ω . So far, the main metrological use of the quantized Hall effect has been for the measurement of electrical resistance with direct current. However, NPL and other laboratories are carrying out research into the quantized Hall effect with alternating current in the hope that this will lead to a new standard of electrical impedance. Just as with the Josephson voltage standard the devices used for realizing R_K have become more sophisticated. Arrays of quantum Hall effect devices now allow realization of a wide range of standard resistance values between $R_K/200$ and $50R_K$. The calibration of resistances with nominal values up to 1 M Ω or down to 1 Ω is possible without using transfer standards of intermediate values, and consequently the uncertainties can be reduced by a factor of 10 or 100 (a few parts in 10^7 for 1 M Ω , one part in 10^9 for 1 Ω) ([Poirier et al. 2002](#)).

5. The third apex of the metrological triangle

(a) *Success of the semi-classical treatment*

In both the Josephson voltage standard and the quantized Hall effect standard of resistance the basic nature of the effects is explained in terms of a macroscopic wave function phase. However, having appealed to quantum mechanics to provide a complex order parameter the phase of this order parameter is then treated as a purely classical variable. It is hard to fault this approach since these simple models explain very straightforwardly the extreme accuracy of the two standards. Nevertheless at a fundamental quantum mechanics level the wave function phase should be treated as an operator with a conjugate variable given by the pair number operator, the two satisfying a commutation relationship

$$[N, \varphi] = i. \quad (5.1)$$

Questions have been asked from the earliest days of the Josephson effects concerning the adequacy of the semi-classical treatment of these effects which assign a precise value to the phase at every point in the devices (see for example [Anderson 1967](#)). The general assumption has been that it is valid to replace the phase operator with a classical phase variable for the situation where the number of

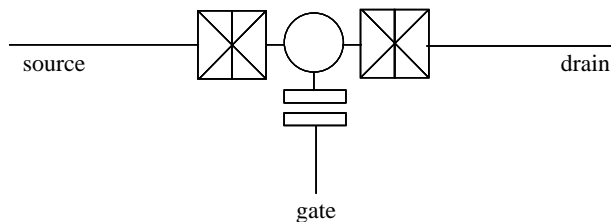


Figure 4. Schematic of single electron transistor.

pairs involved is very large and therefore not well defined. Provided that the system energy is insensitive to quite large pair number fluctuations $\delta N \gg 1$ then the phase fluctuations will become small. This is the justification for the semi-classical approach to both Josephson standard and quantum Hall effect standard. Recent fabrication developments are allowing devices to be produced in which this inequality is no longer clearly satisfied. It is as a result of such developments that a third quantum electrical standard has been proposed and is under development.

(b) *A Possible quantum current standard: the current pump and turnstile*

As sub-micron thin film fabrication techniques became available experiments began to be performed with very small normal metal tunnel junctions. It became clear that a new regime of behaviour would be realized when the junction capacitance C is sufficiently small that, at an operating temperature T the charging energy $E_c = e^2/2C$ for addition of a single fundamental charge leads to an increase in energy which is much greater than the energy of a typical thermal fluctuation $k_B T/2$.

$$k_B T \ll e^2/2C. \quad (5.2)$$

More than a single charge can be induced onto the plates of the capacitor by applying a suitable voltage to a third *gate* electrode, with capacitance C_g between it and one of the other electrodes (see figure 4). The quantized charge Ne on each electrode, induced by the gate electrode voltage, is then no longer subject to thermally driven fluctuations and N becomes a good quantum number. (This effect, known as *Coulomb blockade*, was also coming to the attention of semiconductor scientists as they became able to fabricate complementary metal oxide semiconductor (CMOS) devices which satisfied the same condition, and superconducting Josephson tunnel junctions for which the Cooper pair charge replaced that of singly charged carriers.) Apart from this condition, in order to detect the effects of Coulomb blockade the lifetime of a typical charge state on the capacitor must be long enough to allow its observation. The capacitor must be connected to a source of electric charge and this will have an effective impedance Z . The lifetime of charge fluctuations in this case (and the minimum fluctuation time) $\Delta t \sim ZC$. Using the uncertainty principle relationship the condition becomes

$$\Delta t \cdot \Delta E \geq \hbar,$$

and substituting in this equation leads to the requirement

$$Z \geq \frac{\hbar}{C\Delta E} = \frac{2\hbar}{e^2}. \quad (5.3)$$

Within a factor of order unity this simplified argument shows that any impedance connecting the capacitor to a source of charge must be greater than the quantum of resistance $R_Q = h/e^2$. However, this impedance should not be made excessively large since this will limit the speed of operation of the device. The maximum electron transfer rate is set by around $1/ZC$ per second or a current of $I < e/ZC$.

In practice the usual configuration for such a Coulomb blockade device consists of a small central island of metallic conductor, connected through *two* tunnel junctions to a source and drain for charge. It is these two tunnel junctions which must have impedances exceeding R_Q . For reasons which will become clear shortly a third electrode (gate) is also provided, which allows the island to be controlled by static voltages.

Provided the inequality of equation (5.3) is satisfied the presence of an excess charge on the island between tunnel barriers suppresses strongly the probability that another charge will tunnel onto the island. However, the energy barrier against these processes can be drastically lowered by applying a voltage V_g to the gate electrode. The presence of a d.c. bias voltage V_b across the series connected junctions ensures that tunnelling under this gate voltage condition only occurs in one direction.

The electrostatic energy of the system determines its adiabatic evolution. We define the charge, $Q = Ne$, on the central island. The part of the total electrostatic energy which depends on the number of electrons is

$$E_{\text{el}} = \frac{(Q - Q_{\text{ex}})^2}{2C_{\Sigma}},$$

where the total capacitance of the island is $C_{\Sigma} = (C_L + C_R + C_G)$ and C_R (C_L) is the capacitance with the right (left) electrode whereas C_G is the capacitance to the gate electrode. The induced charge on the island is controlled by the gate voltage in addition to the voltages across the junctions on either side of the island:

$$Q_{\text{ex}} = (V_L C_L + V_R C_R + V_G C_G).$$

The charging energies for adding (Δ^+) or removing (Δ^-) an electron from the island are given by

$$\Delta^{\pm} = E_{\text{el}}(Q) - E_{\text{el}}(Q \pm e) = \mp \frac{e}{C_{\Sigma}} (Q - Q_{\text{ex}} \pm e/2).$$

Thus if $Q_{\text{ex}} = (n + 1/2)e$ the two charge states $Q = ne$ and $Q = (n + 1)e$ have the same energy. As a result, current can flow freely because the system can alternate between the two degenerate states. Away from this degeneracy point the current is blocked as long as

$$eV_b \ll e^2/2C_{\Sigma} \quad \text{and} \quad k_B T \ll e^2/2C_{\Sigma}.$$

There are several sources of error which mean that the device gating is not exactly equal to ne in each period of the applied a.c. gate voltage. These include co-tunnelling events, which involve simultaneous and coherent tunnelling of electrons at two or more junctions, and photon assisted tunnelling in which residual noise processes at microwave frequencies comparable to the unbiased

barrier height can give rise to rare additional electron transfer events. The first of these processes is strongly suppressed by using an array of N identical junctions in series, the a.c. gate voltage being applied to the central island. The second, much rarer, process requires careful attention is paid to the high frequency electromagnetic environment of the junction array as well as the spectral purity of any microwave source which drives it.

Two slightly different forms of single-electron transistor (SET) array have been investigated. The first applies the gate voltage only to the central island in the array, the so-called *turnstile* realization. The second *pump* form applies a sequence of voltages to separate gate electrodes adjoining each individual island in the array. The former is simpler to implement and operate though the latter can be made more accurate for a given number of junctions in the array.

As long ago as 1996 a seven junction electron pump was operated as an electron counter with an error per electron pumped of 15 parts in 10^9 and an average hold time of 600 s (Keller *et al.* 1996, 1998, 1999). The accuracy and hold time are sufficient to enable a new fundamental standard of capacitance. The measured accuracy of the pump has been compared with theoretical predictions as a function of pumping speed and temperature. To maximize the Coulomb blockade and thus minimize errors, the pump must be designed with small junctions to reduce junction capacitance, small islands to reduce island self-capacitance, and a substrate with a small dielectric constant to reduce stray capacitance. For small islands, cross-capacitance to all nearby conductors must also be considered. As well as the main sequence of gate pulses applied to each island a subsidiary pulse with reversed sign and suitably adjusted amplitude is applied to the neighbouring gates to cancel the effects of cross-capacitance. The impressive overall accuracy attained is still significantly lower than theory predicts on the basis of the present understanding of error mechanisms but it is sufficient to allow calibration of a stable capacitor C_0 which is charged up by the pumped electron current over a well-defined number of cycles of the applied gate voltage. Note, however, that the mean current flow in this case is only some pA, a value too small to allow accurate measurement (at the sub-ppm level) against conventional current standards, even using the ingenious cryogenic current comparator (CCC). Recently a Coulomb blockade device, a radio frequency single-electron transistor (RF-SET), has been employed to measure currents by direct counting of time-correlated tunnelling events. This technique may in the future provide the necessary accuracy and bandwidth.

Attempts to realize a true quantum current standard based on these techniques have involved work to increase the maximum frequency f at which pumping with low error rates can occur. To date this has not been increased significantly above 10 MHz but note below there are several promising approaches which are under investigation.

(c) *R-SET pump to allow fewer junctions*

The R-SET pump differs from the conventional SET pump by the addition of resistors at one or both ends of the chain of junctions (see figure 5). These resistors suppress co-tunnelling events in a similar way to the addition of further junctions in series and so should allow the R-SET pump to perform as well as the conventional pump with fewer than seven junctions; it should therefore have the

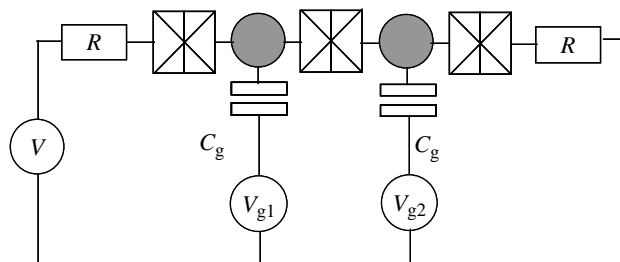


Figure 5. shows a schematic of an RSET-pump device.

advantage of rather higher speed (and consequently higher current operation), and of simplicity of the driving electronics (although at the expense of a more complex fabrication process). Experimental tests of the R-SET pump have recently begun (Feltn *et al.* 2003).

(d) *Expected limits to pump and turnstile performance*

Pekola *et al.* (1999) have calculated the corrections expected from a series array of N Josephson junctions satisfying the charge mode representation criterion that $E_c > E_J$. They find that the errors are rather large when N is small, especially when the ratio $E_J/E_C \geq 0.1$. However, for $N > 7$ and $E_J/E_C \sim 0.03$ the error can be reduced to less than 1 in 10^8 and the maximum frequency before Zener tunnelling transitions to higher energy bands is expected to produce comparable errors is $f_{\max} \sim E_J/\hbar$. To raise f_{\max} to 10 GHz we require $E_J > 2 \times 10^{-5}$ eV, further requiring that $E_C > 2$ meV, a value not yet achieved. Future developments in nanotechnology may allow the capacitance to be reduced sufficiently to achieve this level.

(e) *Surface acoustic wave devices*

A very different form of quantum current standard was proposed (and demonstrated in prototype form) by Shilton *et al.* (1996). The single electron transistor surface acoustic wave (SET-SAW) device is fabricated on a semiconductor substrate (GaAs/Al_xGa_{1-x}As heterostructure) of overall dimensions 2 mm by 8 mm, containing a quasi 2DEG near the surface. An interdigitated transducer at one end of the device produces a surface acoustic wave which propagates past a central region where a constriction in the 2DEG has been formed. The transducers typically have 60 pairs of fingers with a pitch of 1 μ m, operating at a frequency of around 3 GHz. The travelling wave produces a corresponding electrical potential in the piezo-electric GaAs material, which interacts with the 2DEG. In the region of the constriction (usually formed by a metallic split-gate deposited on the surface or an etched channel) the minima of the SAW potential can be regarded as moving quantum wells, which transport electrons through the constricted channel. If the channel is sufficiently closed i.e. ‘pinched-off’ such that normal conduction is prohibited and the potential of the SAW can be arranged such that each potential minimum transports the same (small) number of electrons, the device functions as a current source, generating a current $I = nef$, where n is an integer, e is the electron charge and f is the frequency of the SAW.

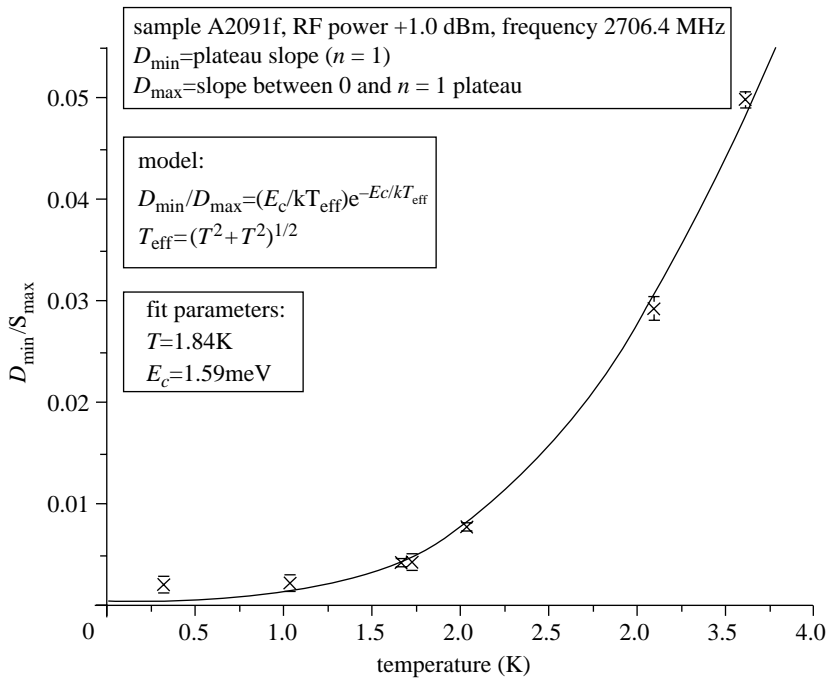


Figure 6. Experimental data on the slope of the current plateaux in a SET-SAW device, as a function of temperature (Fletcher *et al.*).

The state-of-the-art SET-SAW system has been described by Fletcher *et al.* (2003). The experimental set-up consists of a ^3He cryogenic insert, with a sample holder in vacuum, allowing for the variation of the sample temperature between 300 mK and approximately 20 K. Recent experimental work in conjunction with NPL has included the measurement of the slopes of the ‘quantized plateaux’ as a function of temperature (in a genuine quantum standard, the plateaux will have no measurable slope over a reasonable region of parameter space). These results compare well with a quantum mechanical model of the electron transport (Flensberg *et al.* 1999a,b) and suggest that the accuracy of the current quantization is presently limited to worse than the desired one part per million level by an intrinsic electron heating effect. Present research is concentrating on repeating these temperature dependence studies on a variety of samples, and investigating means of improving the accuracy—for example improving the SAW transducer efficiency and using samples with multiple gates to control the channel shape (see figure 6). If the overheating effects can be overcome it has been estimated that the maximum speed of operation would be around 10 GHz, giving a current of some 2 nA, much higher than is currently available from the more accurate SET pumps. At the time of writing the accuracy of SET-SAW devices is no longer limited by the overheating of electrons due to RF power needed by the SAW transducer and by the rate at which the acoustic wave may be turned on and off since very low microwave powers are now required. The accuracy of the effect is such that interactions with impurities can be detected. These interactions lead to new mechanisms of charge transport through the

quantum dot. Improved control of the channel charging energy is expected to lead to improvements in accuracy.

6. Superconducting quantum current standards

Up to this point our discussion of potential quantum current standards has been based on a consideration of singly charged carrier transport under the influence of an oscillating voltage. There exists another class of possible standards which rely on very small Josephson tunnel junctions and pass Cooper pairs rather than single electrons. Although the accuracy so far achieved with these devices is far worse than any SET pump they have some attractions, especially the possibility of higher frequency operation and the appeal of macroscopic quantum coherent operation which make them of continuing interest.

(a) Cooper pair pumps

At its simplest the Cooper pair pump is identical to the SET pump with the tunnel junctions replaced by small capacitance Josephson junctions. The coupling energy of the superconducting order parameter across the junction, E_J , is brought into play as well as the energy scale corresponding to the pair charging energy E_C . In order that the blockade charging effects should dominate current transport through the junction, rather than the Josephson effects, another condition

$$E_J \ll E_C,$$

must be satisfied in addition to those of equations (5.2) and (5.3). This raises the question ‘why would you want to produce Cooper pair junctions with very small E_J when you can make normal junctions with E_J identically zero?’ There are at least two reasons. First the Josephson energy, when finite, makes the problem of bias impedance much simpler than for normal junctions which require lead impedances greater than R_Q . Second the attempt to use the macroscopic quantum coherence of a superconductor to realize a coherent quantum current standard, with potentially much higher accuracy than is available with either type of electron pump is still appealing, especially to the metrology community. The particular advantage is that a higher frequency charge transfer (for a given uncertainty) should be attainable with Cooper pair transport, compared with normal charge transport, in junctions of comparable size (apart from the factor of two arising from the double charge involved in the former case).

Any Cooper pair quantum standard should be operated at a very low temperature so that the quasi-particle density in the superconductors is negligibly small. This means operation at $T/T_c < 0.1$. In addition E_J/E_C must be minimized to suppress Landau–Zener tunnelling processes which can cause transitions to higher bands (essentially losing the restriction on adiabaticity). The condition for this tunnel process to happen depends exponentially on the ratio I_z/I_{dc} (Mullen *et al.* 1988) where I_{dc} is the bias current and I_z is given by

$$I_z = \frac{\pi I_J E_J}{16 E_C}.$$

Note also that the interplay of the two conjugate variables, the phase and the number of Cooper pairs (see below) results in a coherent correction such that the current is no longer exactly given by the relation $I=2ef$ (Pekola *et al.* 1999). Further, the coherent correction is proportional to $\cos \phi$, where ϕ is the phase difference over the whole pump, whereas the supercurrent is proportional to $\sin \phi$, rendering it impossible to choose ϕ to eliminate both of these simultaneously. Here the influence of noise can be beneficial since the resulting suppression of a well defined value for ϕ can give rise to a situation in which $\langle \cos \phi \rangle = \langle \sin \phi \rangle = 0$

(b) *The Cooper pair sluice*

A more recent theoretical proposal by the Finnish group (Niskanen *et al.* 2003) aims to circumvent these problems by introducing a single island Cooper pair *sluice*, coupled to a current source through two controllable d.c. SQUID devices (see figure 7). Although experimental results have not been presented at the time of writing the proposal is ingenious and in principle solves several of the problems identified above. The role of the SQUIDS is to allow the Josephson coupling energy of each SQUID to be independently controlled by time dependent applied magnetic flux. At the same time the gate voltage on the central island is also synchronously varied. The net result is that the maximum frequency at which the sluice may be operated is f where

$$f_{\max} \ll E_c/h \leq \Delta_{\text{BCS}}/h.$$

Δ_{BCS} being the superconducting energy gap parameter. On the basis of continuing to use the tried and tested Al angle deposition method and photolithographic patterning the authors suggest that a single sluice could pump up to 10 Cooper pairs per cycle at a frequency of 50–100 MHz (resulting in a current of 0.1 nA) with an error of less than 0.1 ppm.

As the drive towards nanoscale electronic devices proceeds we may confidently expect that lithographic techniques for patterning superconducting weak links will also achieve reliably smaller feature sizes than the approximately 100 nm to which most laboratories are presently limited. In addition the drive to develop superconducting qubits made from superconductors which possess the maximum T_c may lead to deep sub-micron scale Nb junctions being realisable. If the junction capacitance could be reduced to approximately 1 aF then the ratio E_J/E_c could be reduced to around 0.001 and the coherent transfer of Cooper pairs would be the only significant transfer process. The sluice calculation then predicts that currents of a few nA could be realized with 0.1 ppm accuracy.

(c) *The pair charge shuttle*

Yet another related structure which is potentially capable of realizing a Cooper pair current standard is based on the Cooper pair charge shuttle. This presently hypothetical device has aroused considerable interest over the past two decades (Gallop 1987; Gorelik *et al.* 1998, 2001, Isacsson *et al.* 2002) and, with growing confidence in nanomechanical device fabrication, may be approaching experimental realization.

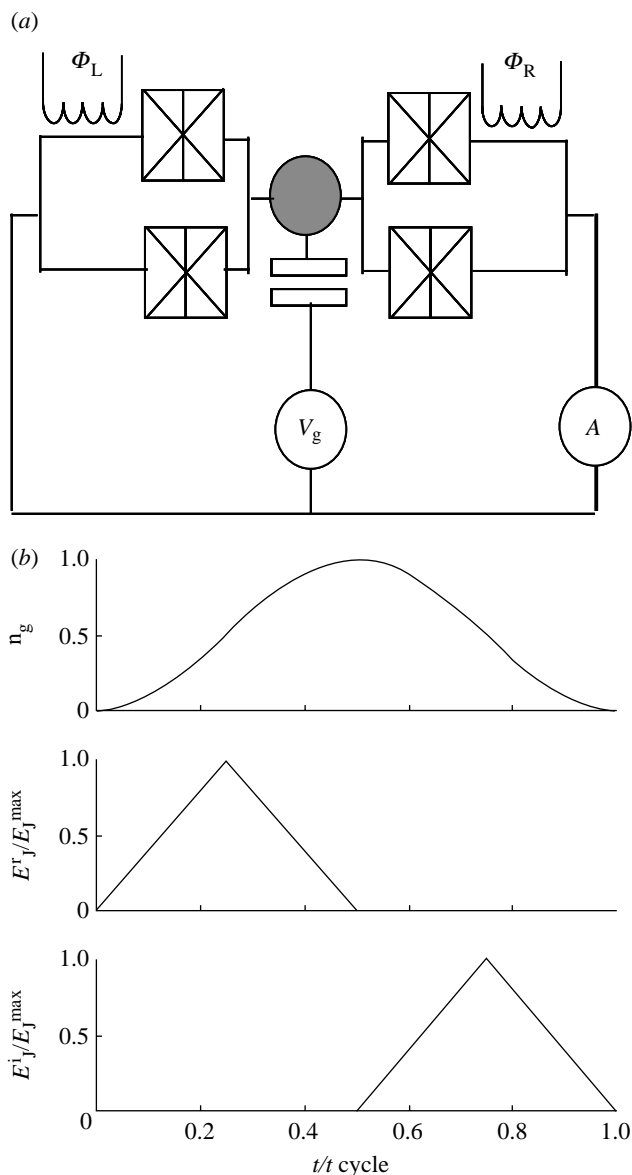


Figure 7. (a) Schematic illustration of the Cooper Pair 'sluice'. The role of the coils is to apply controlled flux pulses through the SQUID loops, and they are synchronized with the periodic gate voltage. (b) The figure below shows the time sequence of applied flux to the two sides of the sluice, together with the gate voltage sequence.

Figure 8 shows a schematic of the mechanical Cooper pair shuttle. A moveable superconducting grain with very low capacitance is placed between two superconducting electrodes. The grain may be moved from one to the other while, at the same time, the voltage on two separate gates may be cyclically switched. When the grain is sufficiently close to one electrode a Cooper pair charge excess may be induced to tunnel to the electrode under suitable gate

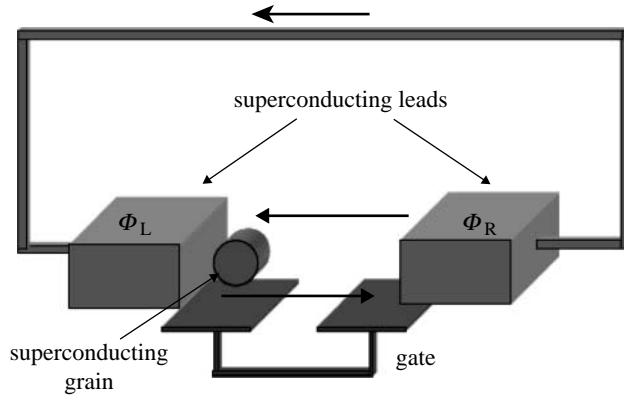


Figure 8. Schematic of moveable grain Cooper pair shuttle (after Gorelik *et al.* 2001).

voltage control. Note that the tunnel probability to the other electrode is exponentially suppressed by the separation distance. When Josephson coupling has allowed the pair to transfer the grain returns to the other electrode to collect another Cooper pair, under control of the other gate. In this way Cooper pairs may be transferred synchronously with the movement of the grain. In this way several of the problems associated with SET pumps, such as co-tunnelling, may be avoided.

7. Bloch oscillations: the quantum dual of the Josephson effect

It has long been recognized, since the pioneering work of Leggett and co-workers (Widom *et al.* 1982; Caldeira & Leggett 1983) that in mesoscopic weakly coupled superconductors there is a quantum conjugate description of a Josephson junction, conjugate that is to the conventional description in terms of a quasi-classical phase difference ϕ between the order parameters in adjacent superconducting regions coupled by pair-transfer tunnelling.

After predictions that the supercurrent through such a Josephson junction would show oscillations at a frequency f and that application of an oscillating voltage at this frequency would give rise to structure in the IV characteristic whenever $f = nI_{dc}/2e$, the conjugate of Shapiro step structure induced in a conventional Josephson junction IVC (Gallop & Radcliffe 1984, 1985; Likharev & Zorin 1985), experimental searches were made for this behaviour. Partially successful observations of the effect were made by Kuzmin & Haviland (1991). Using a single lead-alloy Josephson junction isolated from the environment by high resistance leads they were able to demonstrate under microwave irradiation at frequencies as high as 10 GHz steps at $I = 2ef$ spacing, corresponding to the predicted Bloch oscillations. The slope of the induced ‘steps’ dI/dV in the IVC were far from flat (in fact at high bias frequencies they could only be detected in such a differential conductance plot of dI/dV versus I . This should not surprise us since the ratio $E_J/E_C \sim 1$ and in this regime Landau–Zener excitation to higher bands becomes highly probable.

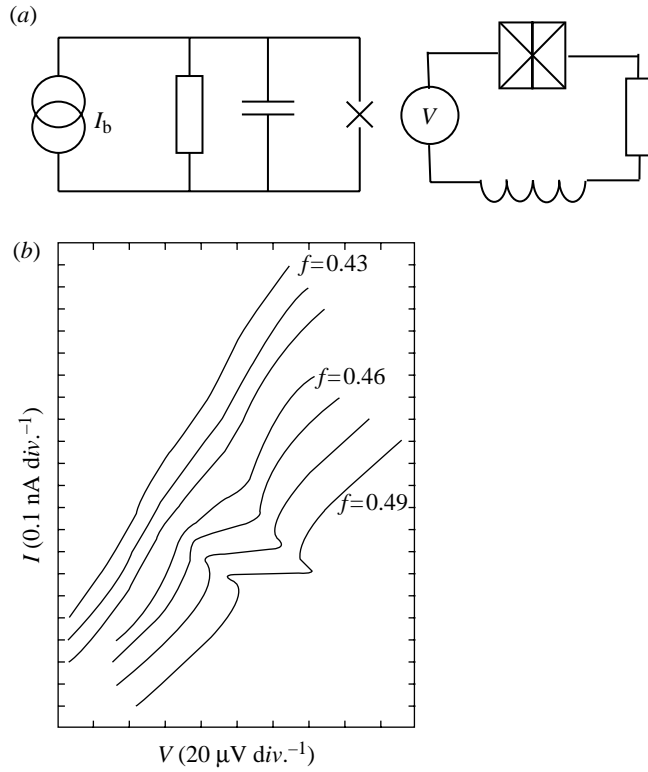


Figure 9. (a) Comparison of RSJ Josephson junction (phase mode) and a voltage biased series resistance Josephson junction (charge mode). (b) IVC of charge mode device (after Haviland *et al.*).

(a) Future Bloch oscillation current standard

There are two significant problems associated with realizing a quantum dual to the Josephson effect voltage standard. The first is associated with achieving a sufficiently low ratio of E_J/E_c to properly localize the pair charges and the second is related to the impedance of the bias leads.

Biasing of such a device is also problematic; Haviland *et al* (2002) have shown that the external impedance of the leads must be greater than R_Q . It is difficult to arrange any transmission line structure which satisfies that criterion. A novel use of a linear array of small area Josephson junctions (actually d.c. SQUID geometry) is proposed in this paper which, through application of magnetic flux can have the line characteristic impedance changed between $\ll R_Q$ and $\gg R_Q$ without introducing a dissipative element. A single small junction with E_J/E_c is situated between two such array bias leads. The IVC may be switched between purely ohmic behaviour when the line impedance is small to that of the ideal Bloch oscillation device in which there is a region of critical voltage at zero bias current so that it appears as a perfect insulator. At higher voltage bias a re-entrant region is seen (as in figure 9b). The behaviour is just as the quantum electrodynamic duality of a Josephson junction. These devices might allow a current standard working up to at least 1 nA to be realized. A further possibility would be to use the unbiased Josephson array analogy to produce a current

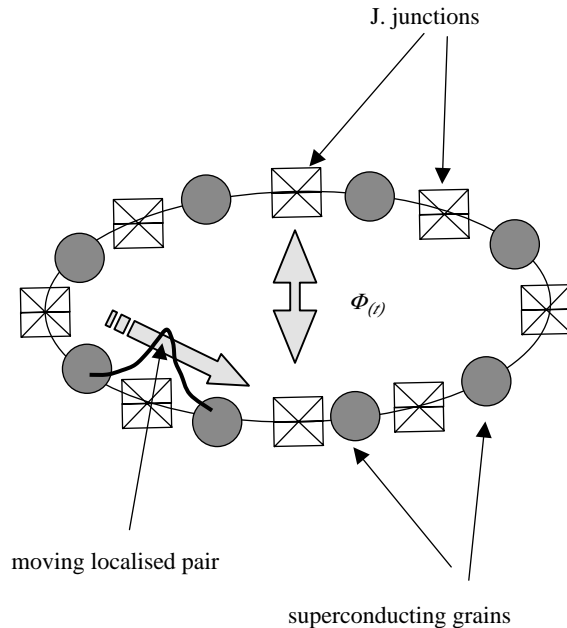


Figure 10. Hypothetical scheme for a Cooper pair ring current standard with alternate small capacitance junctions and superconducting grains. The Cooper pair charge is localized at the junctions and is driven around the ring by an oscillating magnetic flux applied to the ring.

standard which does not require d.c. bias connections. A ring of small identical Josephson junctions in which the kinetic inductance of the individual islands between junctions is greater than the Josephson inductance of each junction provides well localized charge soliton states which can propagate in a lossless fashion around the ring (we assume the temperature is low enough to ignore the influence of quasi-particle excitations). Then provided that the following condition on the dimensionless parameter β_L (the dual of β_C) is satisfied:

$$\beta_L = \frac{2\pi V_c L}{2eR^2} > 1,$$

it should prove possible to pump Cooper pairs *uni-directionally* around the ring synchronously under the influence of an applied purely alternating magnetic flux. In this case one must ask how such an internally generated current might be compared with an external current, for standardizing purposes. Here again the remarkable superconducting precision measurement device, the CCC might have a role to play. If the ring could form part of a winding of a CCC without compromising the impedance requirements (e.g. if a part of the junction ring was replaced by a length of plain superconductor) then the quantized direct current induced by the a.c. magnetic flux could be compared with an external current with high accuracy (figure 10).

8. The zoo of electrical standards

In the preceding sections, we have considered a wide variety of three types of possible electrical standards (voltage, current and resistance) which may be

Table 1. Summary of the range of types of quantum electrical standards

type of standard	voltage fluxons	current electrons	resistance electrons/fluxons
<i>incoherent (stochastic) transfer</i>	flux flow transistor	SET devices	ballistic transport in e.g. carbon nanotubes, even at RT
	vortex in a long Josephson junction	SET-SAW turnstile devices electron pumps	
<i>coherent transfer</i>	shapiro steps	coherent Bloch oscillations	integer quantum Hall effect
	Josephson voltage standard	quantum current standard	fractional quantum Hall effect

Table 2. Comparison of the physical parameters defining the properties of phase and charge representations

parameter (under zero bias)	phase representation	charge representation
potential well depth	$E_J = \Phi_0 I_c / 2\pi$	$E_c = 4e^2 / C$
plasma frequency	$\left(\frac{16\pi I_c}{\Phi_0 C}\right)^{1/2}$	$\left(\frac{16\pi I_c}{\Phi_0 C}\right)^{1/2}$
level width	$2\pi R I_c / \Phi_0$	$2\pi V_c / 2eR$
ratio of level width to level spacing	$Q = \left(\frac{I_c R^2 C}{\Phi_0}\right)^{1/2}$	$Q = \left(\frac{\Phi_0}{I_c R^2 C}\right)^{1/2}$

classified into two distinct forms: incoherent (or stochastic) transfer and coherent transfer. It appears that each electrical standard can be realized in either form and that in general the coherent form is expected (or has been demonstrated) to be the more accurate. Table 1 summarizes the different forms.

(a) Energy scales involved in quantum standards

When considering the different forms summarized in table 1 it is also useful to compare various energy and frequency scales for each standard, expressed as ratios of junction parameter values. Thus the zero bias plasma frequency ω_p (for small oscillations in the (approximately) harmonic potential

$$\hbar\omega_p = (8E_J E_C)^{1/2} = (4\hbar I_c V_c)^{1/2}.$$

The ratio of Josephson energy to Cooper pair charging energy may be written

$$\frac{E_J}{E_c} = \frac{C\Phi_0 I_c}{8\pi e^2}.$$

Both classical potential energy scales and quantum levels (separation and widths) need to be considered and the ratio of level separation to width is included in table 2.

If the energy spacing between quantized plasma frequency levels is greater than the Josephson well depth this implies that the charging energy is greater than the Josephson coupling energy. If the level width is greater than the Josephson well depth and the plasma frequency this means that the semi-classical regime applies

A requirement for successful operation of the unbiased voltage standard arrays is that the individual junctions exhibit hysteresis which implies that the following condition is satisfied:

$$\beta_c = \frac{2\pi I_c R^2 C}{\Phi_0} > 1.$$

This may be explained as the junction charging/discharging time being greater than the period of the Josephson oscillation frequency at the junction critical voltage (i.e. and underdamped junction). This condition can also be seen as corresponding to the energy level width in the phase representation being greater than the energy level width in the charge representation. An underdamped junction may still remain in the adiabatic limit provided the rate of change of bias current $dI_b/dt \ll I_c/RC$

9. Macroscopic quantum effects and electrical standards

(a) *Entangled states and decoherence*

Since the origins of the modern physics revolution at the beginning of the twentieth century the argument about the nature of quantum measurement (QM) and the relationship between classical and quantum regimes has continued. Only within the last decade theorists have begun to propose a detailed resolution of this complementarity principle which rests on the coupling of a quantum system to the multiple degrees of freedom of a classical measuring system. This coupling leads to decoherence of the quantum wave function and explains the ‘collapse of the wavefunction’ which was always the controversial step in the otherwise highly successful Copenhagen interpretation of quantum theory as formalized by von Neumann. Few experiments to test these theoretical predictions have yet been attempted. In the last few years a number of studies have considered the decoherence time applicable to macroscopic states in superconductors. This has been shown to be short compared with, for example the decoherence time for an isolated atom in a trap. On the other hand the superconducting state can be examined much more rapidly than can a sub μK laser-cooled atom in a magneto-optical trap so that the future of quantum computing is expected by many to lie with condensed matter superconducting systems. Heavily isolated Cooper pair box devices or SQUID system qubits could throw light on the exact nature of decoherence in superconductors and help to resolve the QM problem. Developments in superconducting qubit technology have proceeded more or less in step with those in quantum current standards and for the same reason: that ultra-small tunnel junction fabrication techniques were developed in the 1980s. However, the essential entanglement of the former contrasts strongly with the quasi-classical behaviour of the latter. One of the important issues for quantum metrology in the future is to fully understand the differences between these two systems.

Two-level quantum systems capable of existing in a coherent superposition of their quantum states and maintain it for a significant time before it is read out—form the elementary units to perform quantum entanglement. They are the building blocks for a variety of exciting applications, commonly referred to as quantum information processing (QIP) and QM. Implications for metrology are threefold: there is a need to be able to measure the quantum state of a system of quantum bits in a fast, accurate and noiseless way; the hardware for QIP is the same as that for quantum standards (i.e. standards using entanglement); finally, quantum-limited devices (signal-to-noise ratio solely determined by the uncertainty principle) can be built on the same principles.

(b) *Two-level coherent system and the Josephson voltage standard*

At present the more exact form (voltage) of electrical standard relies on the coherence between all the electron pairs in a piece of superconductor. Moving from the usual type of Josephson junction towards one for which the phase difference may no longer be treated as a purely classical variable may introduce possible corrections to the exactness of the fundamental voltage to phase relationship. Consider first a two-level picture of a conventional Josephson junction with a direct voltage bias V across it. The simplest picture describes the system in terms of two energy levels whose separation is proportional to voltage. For a given V the junction emits photons as it makes transitions from the upper to the lower level, with photon energy

$$E = hf = 2 \text{ eV}.$$

In the limits set by equations (5.2) and (5.3) the Josephson coupling energy E_J can be related to the matrix element $A = \langle L | H_{LR} | R \rangle$ between the pair charge being on the left electrode ($|L\rangle$) and it being on the right ($|R\rangle$). We may imagine, though perhaps not realise, a form of voltage biasing in which the weak-link is placed between the plates of a capacitor which carries a large voltage difference between its plates. The Hamiltonian for this two level system now becomes

$$H = (Q_L - Q_R)^2/2C + (Q_L - Q_R)V/2 + H_{LR},$$

where Q_L and Q_R are the operators for the electric charge on left and right electrodes, respectively, and we have assumed that the coupling term between the two electrodes through the weak-link is unaffected by the applied bias voltage. The solution for the eigenenergies E_+ and E_- of this biased two level system is a standard result.

$$E_+ = E_0 - \{A^2 + (eV)^2\}^{1/2},$$

$$E_- = E_0 + \{A^2 + (eV)^2\}^{1/2}.$$

These two expressions are plotted in [figure 11](#). Note that although the eigenenergies tend asymptotically towards the simple linear dependence on V which is predicted by equation (2.3) there are significant departures for $V \sim A/2e$. In principle one might interrogate the eigenvalue separation by enclosing the system in a weakly coupled variable frequency microwave spectrometer which would enable a resonance condition to be established at the Rabi frequency

$$f = [E_+(V) - E_-(V)]/h.$$

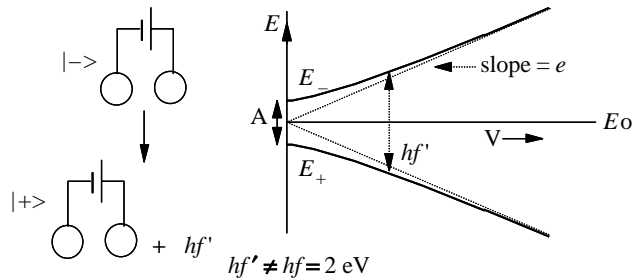


Figure 11. Energy level diagram for voltage biased low- C junction with one pair charge.

This is an extreme example where we suppose that a device with properties towards the Bloch oscillation limit ($E_c > E_J$) continues to exhibit the Josephson effects when it is voltage biased. In view of the absence of clearly observed Bloch oscillations in suitably low C tunnel junctions it might be worth looking for ‘second-order’ evidence for charge coherence by performing a comparison of the voltages across two Josephson junctions irradiated with the same frequency where one junction is in the Bloch limit whereas the other is a large area junction (say $20 \mu\text{m}^2$) of the type used in conventional voltage standards. The maximum voltage difference δV predicted by the above analysis is

$$\delta V < A^2/(e^2 V).$$

Given that the value of A must also be sufficient to prevent thermal fluctuations wiping out coherent coupling between the superconducting electrodes and that an operating temperature of approximately 10 mK is the lowest reasonably achievable sets the condition

$$A/e \gg kT/2e \sim 3 \times 10^{-6},$$

so that with $V \sim 20 \mu\text{V}$ (corresponding to the first microwave step for a frequency of 10 GHz)

$$\delta V < 0.5 \mu\text{V}.$$

Since voltage differences in low inductance superconducting circuits some 10 orders of magnitude smaller than this can be readily detected with a SQUID, this type of experiment may be promising. (A small resistance should be included in the entirely superconducting measurement loop, to avoid phase continuity complications, unlike the arrangement used by Tsai *et al.* 1983.) A null result, in which no voltage-dependent voltage difference is detected between the two types of tunnel junction, is also challenging since it remains necessary to explain what process suppresses quantum coherence effects so effectively. Dissipation, which is completely ignored in this simplified treatment, or the presence of fluctuations introduced via the bias leads, or some stray shunt impedance across the small-area junction may singly or collectively provide possible explanations for the absence of the predicted effect. But if these parameters could be systematically varied while searching for signs of finite δV we might learn a great deal about the influences on decoherence in condensed matter systems. It would also be desirable to understand both biasing of the junction and measurement of the voltage in quantum mechanical terms. It may be that the suppression of quantum coherence results from use of a measurement

technique which amounts to making rapid successive measurements of the quantum state of the junction, forcing it into a state which is not a stationary state for the isolated junction. The measurement process, if rapid enough, may then retain this state in the same way that coherent oscillation has been suppressed in optical experiments, see the so-called ‘Quantum Zeno’ experiment, G. Hackenbroich *et al.* (1998).

10. The electrical triangle: are there corrections to e and h from condensed matter interactions?

The overall aim of the quantum metrological triangle experiments is to verify with a very low uncertainty the coherency of the deduced values of the constants involved in these three quantum phenomena or, in other words, to confirm that these condensed matter physics phenomena, in which inter-particle interactions are undoubtedly strong, yield the free-space values of constants $2e/h$, h/e^2 and e . The target uncertainty needs to be around one part in 10^8 . If there is no deviation, our confidence on the three phenomena to provide us with $2e/h$, h/e^2 and e will be considerably enhanced. Any robust discrepancy will prompt further experimental and theoretical work.

There are other approaches to testing the environmental dependence of the fundamental constants e and h . The accuracy with which these two constants have been determined through the evaluation of other physical measurements are summarized in the best values for the constants which are published by CODATA at regular intervals. The most recent analysis suggests that the values of e and h , as deduced from the rest of physics, do not differ by more than 2×10^{-8} from the values deduced from the assumed values of the constants K_J and K_R . However, to compare directly the value of $2e/h$ and e^2/h from our two established quantum electrical standards would require a better value for the realization of the ampere. At present this is limited to around 2×10^{-7} so, until each vertex of the quantum metrological triangle can be evaluated with precision higher than this no further direct tests can be made. Note that R_K can be written in terms of the fine structure constant α

$$R_K = \frac{h}{e^2} = \frac{\mu_0 c}{2\alpha}.$$

Since both μ_0 and c are defined quantities there is a very direct link between R_K and α . Experiments from the rest of physics provide a best value of α which is in agreement with the value of R_K to within two parts in 10^8 (Flowers 2004)

Still other indirect tests can allow us to make more stringent estimates. As described above, the material independence of the voltages induced on Josephson junctions made from different superconductors when irradiated with the same frequency and biased on the equivalent Shapiro step suggests that the ratio $2e/h$ is material independent at the level of around one in 10^{16} (Tsai *et al.* 1983). A similar test of the material independence of the von Klitzing constant (Hartland *et al.* 1991; Jeanneret *et al.* 1995) shows that the impedance of a Si MOSFET agrees with that of a GaAs heterostructure 2DEG at the level of one in 10^{10} when they are fully quantized on the same plateau. The recent international

comparisons of complete Josephson effect and quantum Hall effect systems show a high level of consistency: from one part in 10^{-10} to a few 10^{-9} .

When considering the theoretical position it is clear that thermodynamic arguments carry more weight than microscopic theory. Thus, when asking whether the Josephson constant $K_J = 2e/h$ exactly Bloch (1970) and Fulton (1973) considered one or more Josephson junctions in a superconducting loop to which a linear flux ramp was applied. The Φ_0 periodicity of the free energy of the ring arises from the (global) application of the relationship

$$\nabla\phi = \frac{2e}{\hbar} A.$$

The requirement that the contour integral of $\nabla\phi$ within the ring gives rise to flux quantization and shielding of external applied magnetic fields. A material variation in K_J would give rise to a difference in the flux quantum between different superconductors. Fulton (1972) has pointed out that since the magnetic flux in a closed superconducting circuit is a conserved quantity, any dependence of K_J on materials, experimental conditions, or other non-exotic variables will violate Faraday's law.

Similar arguments have been deployed to reinforce the accuracy of the relationship $R_K = h/e^2$. Laughlin (1981) used a gauge argument to show that, for a closed 2DEG ribbon with radial magnetic field a single electron per Landau level is transferred from one edge of the loop to the other for each addition of a magnetic flux quantum h/e through the loop. Both the integral and fractional quantum Hall effects are manifestations of new quantized states in the 2DEG, analogous to the quantized flux states in superconductors. At present no similar thermodynamic or quantization arguments have been given to justify a lack of condensed matter correction to a quantized current standard. Thermodynamic arguments are stronger than those based on microscopic physics but the only convincing arguments come from experimental results.

11. Electrical metrology based on magnetic flux and electric charge

Electrical metrology has traditionally treated voltage and current as continuous classical variables. There is now apparent a drive towards measuring quanta rather than continuous variables and this originates from the drive towards nanotechnology. For example the continuing decrease in the size of CMOS gates means that within a few years the number of charges associated with a gate operation will be reduced to single figures. Similarly improvements in material quality combined with scale reduction means that ballistic conduction is becoming apparent, leading to improved power handling. The exploitation of single particle effects such as single electron transistors, spintronics and molecular gates are further developments in the same direction. QIP using condensed matter circuits, based on mesoscopic quantum states, may also become of great practical importance. Thus it may be that metrology in terms of the quantum conjugate variables of electric charge and magnetic flux will be of increasing significance in future. The electrical quantum triangle of standards will be seen to have anticipated these needs.

12. Conclusions

The accuracy of the Josephson voltage–frequency relationship, the absence of observed effects associated with Bloch oscillations and the significance of macroscopic superconducting circuits for investigating fundamental aspects of quantum theory are three related topics which are still not clearly understood. We point out that other types of incoherent quantum standards employing weak superconductivity also exist, which seem to be of intrinsically far lower precision. Finally we propose a sensitive comparison of the microwave induced step voltages of two Josephson junctions with capacitances in two different regimes for which second-order differences may indicate the presence of MQC effects.

Speculating on the future, the requirement for electromagnetic measurements on ever smaller length scales, combined with realizations of quantum circuits, may lead to a rewriting of the fundamentals of electrical metrology. Thus we have already seen that for ballistic conduction and for the more exotic transport properties exhibited by the quantum electrical standards we have outlined electric charge and magnetic flux are more natural (quantum conjugate) variables to describe and monitor their behaviour. The electron pump as a means of calibrating a capacitor already hints at the type of measurement that will be possible and even demanded in a future nanoscale world.

My thanks to many colleagues at NPL, who have tried to help me to better understand this complex topic, with special thanks to Alexander Tzalenchuk, Brian Petley, J. T. Janssen and Jonathan Williams.

References

- Anderson, P. W. 1967 *Prog. Low Temp. Phys.* **5**, 1–43.
- Benz, S. P., Hamilton, C. A., Burroughs, C. J., Harvey, T. E. & Christian, L. A. 1997 Stable 1 volt programmable voltage standard. *Appl. Phys. Lett.* **71**, 1866–1868.
- Benz, S. P., Dresselhaus, P. D. & Burroughs, C. J. 2001 Nanotechnology for next generation Josephson voltage standards. *IEEE Trans. Instrum. Meas.* **50**, 1513–1518.
- Bloch, F. 1970 Josephson effect in a Superconducting Ring. *Phys. Rev. B* **2**, 109–121. (doi:10.1103/PhysRevB.2.109.)
- Caldeira, A. O. & Leggett, A. J. 1983 Influence of dissipation on quantum tunneling in macroscopic systems. *Phys. Rev. Lett.* **46**, 211–214. (doi:10.1103/PhysRevLett.46.211.)
- Feltin, N., Devoille, L., Piquemal, F., Lotkhov, S. & Zorin, A. 2003 *IEEE Trans. Instrum. Meas.* **52**, 599–603.
- Flensberg, K., Niu, Q. & Pustilnik, M. 1999 Nonadiabaticity and single-electron transport driven by surface acoustic waves. *Phys. Rev. B* **60**, R16 291–R16 294.
- Flensberg, K., Odintsov, A. A., Liefink, F. & Teunissen, P. 1999 *Inter. J. Mod. Phys. B* **13**, 2651.
- Fletcher, N. E., Ebbecke, J., Janssen, T. J. B. M., Ahlers, F. J., Pepper, M., Beere, H. E. & Ritchie, D. A. 2003 Quantized acoustoelectric current transport through a static quantum dot using a surface acoustic wave. *Phys. Rev. B* **68**, 245 310.
- Flowers, J. 2004 The route to atomic and quantum standards. *Science* **306**, 1325–1330.
- Fulton, T. A. 1973 Implications of solid-state corrections to the Josephson voltage-frequency relation. *Phys. Rev. B* **7**, 981–982. (doi:10.1103/PhysRevB.7.981.)
- Gallop, J. C. 1987 Macroscopic quantum coherence in a charge mode device. *IEEE Trans. Mag. MAG* **23**, 1158.
- Gallop, J. C. & Radcliffe, W. J. A. 1984 superconducting quantum current standard? NPL Report QU67.

- Gallop, J. C. & Radcliffe, W. J. 1985 A phenomenological model of pair and fluxon transfer in superconducting weak-links. *Phys. Lett. A* **112A**, 74–76.
- Gorelik, L. Y., Isacsson, A., Voinova, M. V., Kasemo, B., Shekhter, R. I. & Jonson, M. 1998 Shuttle mechanism for charge transfer in coulomb blockade nanostructures. *Phys. Rev. Lett.* **80**, 4526–4529.
- Gorelik, L. Y., Isacsson, A., Galperin, Y. M., Shekhter, R. I. & Jonson, M. 2001 Coherent transfer of Cooper pairs by a movable grain. *Nature* **411**, 454–457.
- Hackenbroich, G., Rosenow, B. & Weidenmüller, H. A. 1998 Quantum zeno effect and parametric resonance in mesoscopic physics. *Phys. Rev. Lett.* **81**, 5896–5899.
- Hartland, A., Jones, K., Williams, J. M., Gallagher, B. L. & Galloway, T. 1991 Direct comparison of the quantized Hall resistance in gallium arsenide and silicon. *Phys. Rev. Lett.* **66**, 969–973.
- Haviland, D. B., Watanabe, M., Agren, P. & Andersson, K. 2002 Quantum complementarity for the Superconducting Condensate and the Resulting Electrodynamic Duality. *Phys. Scripta* **102**, 62–68.
- Isacsson, A., Gorelik, L. Y., Shekhter, R. I., Galperin, Y. M. & Jonson, M. 2002 Mechanical Cooper pair transportation as a source of long-distance superconducting phase coherence. *Phys. Rev. Lett.* **89**, 277 002.
- Jain, A. K., Lukens, J. E. & Tsai, J. S. 1987 Test for relativistic gravitational effects on charged particles. *Phys. Rev. Lett.* **58**, 1165–1168.
- Jeanneret, B., Jeckelmann, B., Bulmann, H. J., Houdre, R. & Ilegems, M. 1995 Influence of the device width on the accuracy of quantization in the integer quantum Hall effect. *IEEE Trans. Instrum. Meas.* **44**, 254–257.
- Keller, M. W., Martinis, J. M., Zimmerman, N. M. & Steinbach, A. H. 1996 Accuracy of a electron counting using a 7 junction electron pump. *Appl. Phys. Lett.* **69**, 1804–1806.
- Keller, M. W., Martinis, J. M. & Kautz, R. L. 1998 Rare errors in a well-characterized electron pump: comparison of experiment and theory. *Phys. Rev. Lett.* **80**, 4530–4533.
- Keller, M. W., Eichenberger, A. L., Martinis, J. M. & Zimmerman, N. M. 1999 A capacitance standard based on counting electrons. *Science* **285**, 1706–1709.
- Klushin, A. M., Behr, R., Numssen, K., Siegel, M. & Niemeyer, J. 2002 Accurate measurements of quantum voltage steps on arrays of bicrystal Josephson junctions. *J. Appl. Phys.* **80**, 1972–1979.
- Kohlmann, J., Behr, R. & Funck, T. 2003 Josephson voltage standards. *Meas. Sci. Technol.* **14**, 1216–1228.
- Krasnopolin, I. Y., Behr, R. & Niemeyer, J. 2002 Highly precise comparison of Nb/Al/AlO_x/Al/AlO_x/Al/Nb Josephson junction arrays using a SQUID as a null detector. *Supercond. Sci. Technol.* **15**, 1034–1036. (doi:10.1088/0953-2048/15/7/306.)
- Kuzmin, L. S. & Haviland, D. B. 1991 Observation of the Bloch oscillations in an ultrasmall Josephson junction. *Phys. Rev. Lett.* **67**, 2890–2893.
- Laughlin, R. B. 1981 Quantized Hall conductivity in two dimensions. *Phys. Rev. B* **23**, 5632–5633. (doi:10.1103/PhysRevB.23.5632.)
- Likharev, K. K., Zorin, A. B. & Low, J. 1985 *Temp. Phys.* **59**, 347.
- Mullen, K., Ben-Jacob, E. & Schuss, Z. 1988 Combined effect of Zener and quasiparticle transitions on the dynamics of mesoscopic Josephson junctions. *Phys. Rev. Lett.* **60**, 1097–1100.
- Nam, S., Benz, S., Dresselhaus, P. D. & Martinis, J. 2003 Johnson noise thermometry measurements using a quantized voltage noise source for calibration. *IEEE Trans. Instrum. Meas.* **52**, 550–554.
- Pekola, J. P., Toppari, J. J., Aunola, M., Savolainen, M. T. & Averin, D. V. 1999 Adiabatic transport of Cooper pairs in arrays of Josephson junctions. *Phys. Rev. B* **60**, 9931–9934.
- Poirier, W., Bounouh, A., Hayashi, K., Fhima, H., Piquemal, F., Genevès, G. & André, J. P. 2002 *J. Appl. Phys.* **92**, 2844–2854.
- Silton, J. M., Talyanskii, V. I., Pepper, M., Ritchie, D. A., Frost, J. E. F., Ford, C. J. B., Smith, C. G. & Jones, G. A. C. 1996 High frequency single electron transport in a quasi-one dimensional GaAs channel induced by surface acoustic waves. *J. Phys. Condens. Matter* **8**, L531–L539.

- Taylor, B. N., Parker, W. H. & Langenberg, D. N. 1969 Determination of e/h , using macroscopic quantum phase coherence in superconductors: implications for QED. *Rev. Mod. Phys.* **41**, 375–496.
- Tsai, J. S., Jain, A. K. & Lukens, J. E. 1983 High precision test of the universality of the Josephson voltage–frequency relation. *Phys. Rev. Lett.* **51**, 316–319.
- Von Klitzing, K. 2005 Developments in the Quantum Hall effect. *Phil. Trans. R. Soc. A* **363**. (doi:10.1098/rsta.2005.1640.)
- von Klitzing, K., Dorda, G. & Pepper, M. 1980 New method for high-accuracy determination of the fine-structure constant based on quantized Hall resistance. *Phys. Rev. Lett.* **45**, 494–497. (doi:10.1103/PhysRevLett.45.494.)
- Widom, A., Megaloudis, G., Clark, T. D., Prance, H. & Prance, R. J. 1982 *J. Phys. A* **15**, 3877.
- Williams, J. M., Janssen, T. J. B. M., Palafox, L., Humphreys, D. A., Behr, R., Kohlmann, J. & Müller, F. 2004 The simulation and measurement of the response of Josephson junctions to optoelectronically generated short pulses. *Supercond. Sci. Technol.* **17**, 815–818.